



Fermilab

The Effects of Landau Cavities in the Energy Doubler - Bunch Length, Microwave Instability and Single Bunch Instability

King-Yuen Ng

March, 1982

I. INTRODUCTION

Due to wall impedance, space-charge impedance and cavities, a bunch will exhibit bunch-shape oscillations with frequencies of the order of that of the synchrotron oscillation.¹ The most natural way to stabilize these oscillations is to employ Landau damping. The external radio frequency (RF) force enforcing the synchrotron motion in a stationary bucket is

$$F = eV_{RF} \sin\phi, \quad (1.1)$$

where V_{RF} is the peak voltage per turn, e the particle charge and ϕ the RF phase angle measured from the synchronous position. The RF potential is therefore

$$U = -eV_{RF} \cos\phi, \quad (1.2)$$

which is very nearly harmonic for small half bunch length ϕ_m . As a result, the synchrotron frequency has very small spread

$$\begin{aligned} \frac{\Omega_s}{\Omega_{s0}} &= \frac{\pi}{2} \frac{1}{K(\sin^2 \phi_m/2)} \\ &\approx 1 - \frac{\phi_m^2}{16} - \frac{23}{3072} \phi_m^4 + \dots, \end{aligned} \quad (1.3)$$

where Ω_{S0} is the synchrotron frequency for zero bunch length and $K(\sin^2 \phi_m/2)$ is the complete elliptic integral of the first kind*. Taking the Doubler as an example, with $V_{RF} = 2.16$ MV per turn, at extraction energy of $1000 \text{ GeV}/c^2$, the spread is only 0.6% ($\phi_m \sim 0.3$ rad.) and at injection energy of $150 \text{ GeV}/c^2$, the spread is 1.6% ($\phi_m \sim 0.5$ rad.).

A method to enlarge the spread of the synchrotron frequency is to add higher harmonic cavities, commonly called the Landau cavities, such that the RF force becomes

$$F = eV_{RF}(\sin\phi - k\sin m\phi) \quad (1.4)$$

and the corresponding RF potential is

$$U = -eV_{RF}(\cos\phi - \frac{k}{m} \cos m\phi). \quad (1.5)$$

In above, k , the ratio of the Landau cavity voltage to the RF cavity voltage, has to be small so that the effective RF voltage will not differ by too much from the original RF voltage. Also, m should be or very near to an integer so that the effect of the Landau cavities to each RF bucket will be nearly the same.

The addition of the Landau cavities leads to bigger deviation from the harmonic well and therefore bigger spread in Ω_S . For the extreme case of $km = 1$, the ϕ^2 term drops out from the potential leaving

$$U = \frac{m^2-1}{24} eV_{RF} \phi^4 + \dots \quad (1.6)$$

when ϕ is small, and Ω_S is directly proportional to ϕ_m

$$\frac{\Omega_S(\phi_m)}{\Omega_{S0}} = \frac{\pi}{2} \left(\frac{m^2-1}{6} \right)^{\frac{1}{2}} \frac{\phi_m}{K(\frac{1}{2})}, \quad (1.7)$$

* $K(x) = \int_0^{\pi/2} d\theta (1-x \sin^2\theta)^{-\frac{1}{2}}$

where $K(\frac{1}{2})$ is the complete elliptic integral of the first kind. In other words, the spread is now 100%.

Several people have advocated that the old CEA cavities be used in the Doubler as Landau cavities. These cavities were originally operated at 475 MHz which is very close to nine times the Doubler RF of 53.1 MHz. The purpose of this note is to estimate the change in bunch length, microwave instability and single bunch dipole oscillation instability when these cavities are turned on. Throughout this note, the extreme case $k_m = 1$ is assumed. We find that (1) bunch length increases if it is short but decreases instead if it is long; (2) the microwave stability limit is nearly unaffected and (3) the single bunch dipole oscillation is stabilized by a great deal. Similar analyses have been made for the Main Ring of Fermilab by S. Ohnuma¹ and for the ISR of CERN by F. Sacherer³. Finally, we study the effects of varying m but keeping $k_m = 1$.

II. HAMILTONIAN, WALL INDUCTANCE AND FREQUENCY SPREAD

II.1 For a particle in a stationary bucket, the Hamiltonian is

$$H = \frac{1}{2} a (\Delta E)^2 + \frac{\omega_0}{2\pi} U(\phi) \quad (2.1)$$

with

$$a = \frac{|\eta| h \omega_0}{\beta^2 E} \quad (2.2)$$

and the effective RF potential given by

$$U(\phi) = -eV_{RF} \left(\cos \phi - \frac{k}{m} \cos m\phi \right). \quad (2.3)$$

In above, ΔE and ϕ , the energy and RF phase in excess of those of the synchronous particle are taken as canonical variables, $h = 1113$ is the harmonic number of the RF system, $\omega_0/2\pi$ is the revolution frequency of the synchronous particle around the ring, β is its velocity in terms of the

velocity of light c , and $\eta = \gamma_T^{-2} - \gamma^{-2}$ is the frequency flip factor with γ_T the transition energy of the ring in terms of the energy of the particle at rest.

At frequencies comparable to the RF, the wall of the beampipe is inductive introducing a longitudinal electric field E_W at the bunch

$$E_W = - \frac{L}{2\pi R} \frac{\partial I_{in}}{\partial t}, \quad (2.4)$$

where L is the total wall inductance and R is the mean radius of the Doubler ring. The instantaneous current I_{in} is given by

$$I_{in} = eN\beta c\lambda \quad (2.5)$$

with N the number of particles in the bunch and λ the linear particle density normalized to unity

$$\int_{\text{bunch}} \lambda(\phi, t) \frac{R}{h} d\phi = 1. \quad (2.6)$$

Due to this inductance, the energy of the particle increases at the rate

$$\frac{d}{dt} \Delta E = \frac{\omega_0 L e^2 N h \beta^2 c^2}{2\pi R} \frac{\partial \lambda}{\partial \phi}. \quad (2.7)$$

If we choose an elliptical distribution of the particles in the longitudinal phase space

$$f(\Delta E, \phi) \propto \left[\Delta E(\phi)_{\max}^2 - \Delta E^2 \right]^{\frac{1}{2}} \quad (2.8)$$

with $\Delta E(\phi)_{\max}$ the maximum of ΔE at ϕ , the linear line density can easily be shown as

$$\lambda = \frac{h}{2RD_m} \left[\cos \phi - \cos \phi_m - \frac{k}{m} (\cos m\phi - \cos m\phi_m) \right] \quad (2.9)$$

where

$$D_m = \sin \phi_m - \phi_m \cos \phi_m - \frac{k}{m} \left(\frac{\sin m \phi_m}{m} - \phi_m \cos m \phi_m \right) \quad (2.10)$$

and ϕ_m is the half bunch length in RF radians. Thus $\partial D / \partial \phi$ is proportional to $\partial U(\phi) / \partial \phi$. The effect of the inductive wall can therefore be conveniently included in Eq. (2.1) by introducing an effective RF voltage V^* :

$$H = \frac{1}{2} a (\Delta E)^2 + \frac{\omega_0}{2\pi} U^*(\phi), \quad (2.11)$$

$$U^*(\phi) = -eV^* (\cos \phi - \frac{k}{m} \cos m\phi), \quad (2.12)$$

where the effective RF voltage is defined as

$$\frac{V^*}{V_{RF}} = 1 - \frac{eNh^2 3c}{2RV_{RF} D_m} \left| \frac{Z}{n} \right|_{ind} \quad (2.13)$$

and the inductive impedance per harmonic in the RF region is

$$\left| \frac{Z}{n} \right|_{ind} = \omega_0 L. \quad (2.14)$$

In a previous note⁴, our estimate for the Doubler was $|Z/n|_{ind} \sim 5$ ohms both at injection and extraction energies in the RF region (Figures 1 and 2). This inductance mainly comes from the resistivity of the beampipe wall, the surfaces of the laminations of the extraction Lambertsons, injection Lambertsons and abort Lambertsons, each contributing nearly equally. If we take the number of protons per bunch as $N = 2 \times 10^{10}$, $R = 10^5$ cm, $V_{RF} = 2.16$ MV, $n = .0028$. and bunch area $S = 0.3$ eV-sec, then as computed in the next section, the half bunch lengths are 0.51 (0.50) and 0.32 (0.35) at injection energy $150 \text{ GeV}/c^2$ and extraction energy $1000 \text{ GeV}/c^2$ respectively when the Landau cavities are turned off (on) and $m = k^{-1} = 9$. The effective RF voltage V^* is reduced from V_{RF} by 3.2% (3.4%) and 12.7% (14.0%) respectively according to Eq. (2.13). The reduction

will be more significant at higher energies and higher beam currents.

II.2 The angular frequency Ω_s of the synchrotron oscillation at amplitude ϕ_0 is given by

$$\frac{\pi}{2\Omega_s} = \int_0^{\phi_0} \frac{d\phi}{a\Delta E(\phi)}, \quad (2.15)$$

using an equation of motion of the Hamiltonian (2.11) from which

$$\Delta E(\phi) = \left\{ \frac{\omega_0}{a\pi} \left[U^*(\phi_0) - U^*(\phi) \right] \right\}^{\frac{1}{2}}. \quad (2.16)$$

The results are shown in Figure 3 with $m = 9$ and different values of k . The abscissa is the ratio of the bunch area to the bucket area with $k = 0$ so that it is independent of the effective RF voltage. When $k = 0$, or when the Landau cavities are turned off, Eq. (2.15) can be integrated exactly to give Eq. (1.3). When k is increased to $1/9$, we see that Ω_s starts from zero and has a spread of 100%.

III. BUNCH LENGTH

From the Hamiltonian (2.11), the bunch area S can be computed

$$S = \frac{8R}{hc} \left[\frac{2EeV^*(\phi_m)}{\pi|\eta|h} \right]^{\frac{1}{2}} M(\phi_m)$$

where

$$M(\phi_m) = \int_0^{\pi/2} dx \sin^2 \frac{1}{2} \phi_m \cos^2 x (1 - \sin^2 \frac{1}{2} \phi_m \sin^2 x)^{-\frac{1}{2}} \left(1 - \frac{k}{m} \frac{\sin^2 \frac{1}{2} m\phi_m - \sin^2 \frac{1}{2} m\phi}{\sin^2 \frac{1}{2} \phi_m - \sin^2 \frac{1}{2} \phi} \right)^{\frac{1}{2}}$$

with

$$\sin \frac{1}{2} \phi = \sin \frac{1}{2} \phi_m \sin x.$$

When the Landau cavities are turned off, $M(\phi_m)$ can be readily integrated to

give

$$M(\phi_m) = E(\sin^2 \frac{1}{2} \phi_m) - \cos^2 \frac{1}{2} \phi_m K(\sin^2 \frac{1}{2} \phi_m),$$

where K and E are complete elliptic integrals of the first kind and second kind respectively. Otherwise, numerical integration is necessary unless $\phi_m \ll 1$. Thus, given a bunch area in eV-sec, the half bunch length ϕ_m can be computed as a function of $N|Z/n|_{ind}$. The results are plotted in Figures 4 and 5 for various values of S at both injection and extraction energies. We see that, for a short bunch, Landau cavities lengthen the bunch. However, starting from $\phi_m \sim .48$ rad, the bunch is shortened instead. This is very obvious if we look at the RF potential in Figure 6. When ϕ is small, the potential with the Landau cavities on is flattened and therefore leads to the lengthening of the bunch. However, when ϕ is small, the potential with the Landau cavities on becomes steeper. This implies that changing ϕ by a little will increase ΔE by a lot. The bunch area, being constant, will be compressed from a circle to a shape that is nearly square; thus the bunch is shortened. We can also see from Figure 6 that the energy spread is always decreased when the Landau cavities are switched on.

In our derivation, the switching on of the Landau cavities is assumed to be adiabatic; the bunch area is therefore unchanged. However, in Sacherer's derivation³, where he was considering an electron machine, the energy spread was assumed unchanged when the Landau cavities were turned on.

IV. MICROWAVE INSTABILITY

IV.1 The Keil-Schnell criterion for microwave stability is

$$\left| \frac{Z}{n} \right|_{MW} < F \frac{|n|}{eE} \frac{(\Delta E)_{FWHM}^2}{I_{in}}, \quad (4.1)$$

where F is a form factor, ~ 0.64 for elliptical distribution and $I_{in} = eN\beta c\lambda$ is the instantaneous current. With elliptical distribution, we obtain

$$\frac{(\Delta E)_{FWHM}^2}{I_{in}} = \frac{3\beta^2 E e v^* D_m}{\pi^2 |n| h I_{AV}}, \quad (4.2)$$

which is independent of the position along the bunch. The average total current for h bunches is

$$I_{AV} = \frac{e N h \omega_0}{2\pi}. \quad (4.3)$$

Thus the stability criterion reduces to

$$\left| \frac{Z}{n} \right|_{MW} \leq \frac{3\beta^2 v^* (\phi_m) D_m F}{\pi^2 h I_{AV}}. \quad (4.4)$$

If we define

$$r = \frac{|Z/n|_{ind}}{|Z/n|_{MW}}, \quad (4.5)$$

where $|Z/n|_{ind}$ is the inductive impedance at RF frequencies, the critical number of particles per bunch N_c is given by

$$N_c \left| \frac{Z}{n} \right|_{MW} = \frac{2R V_{AF} D_m}{e h^2 \beta c} \frac{3\beta^2 F r / \pi}{1 + 3\beta^2 F r / \pi}. \quad (4.6)$$

For the Doubler, $|Z/n|_{ind} \sim 5$ ohms and $|Z/n|_{MW} \sim 1$ ohm; thus $r \sim 5$. However, in Eq. (4.6), given the bunch area S , D_m , being dependent on ϕ_m , will depend on N_c also. Thus Eq. (4.6) can be solved numerically only. The results are plotted in Figure 7. As an example, at $r = 5$, $S = 0.3$ eV-sec., the stability limits are, at $150 \text{ GeV}/c^2$,

$$N_c \left| \frac{Z}{n} \right|_{MW} = \begin{cases} 1.29 \times 10^{11} \text{ ohms} & \text{Landau cavities off} \\ 1.31 \times 10^{11} \text{ ohms} & \text{Landau cavities on} \end{cases}$$

and, at $1000 \text{ GeV}/c^2$,

$$N_C \left| \frac{Z}{n} \right|_{MW} = \begin{cases} 3.12 \times 10^{11} \text{ ohms} & \text{Landau cavities off} \\ 3.01 \times 10^{11} \text{ ohms} & \text{Landau cavities on .} \end{cases}$$

Thus the changes with Landau cavities are not significant.

Remarks

1. When Landau cavities are switched on, the critical stability limit $N_C |Z/n|_{MW}$ changes by less than 10% in all cases under investigation. This is because

$$N_C \left| \frac{Z}{n} \right|_{MW} \propto \frac{(\Delta E)^2}{I_{in}} \propto \phi_m (\Delta E)_M^2, \quad (4.7)$$

where ΔE_M is the maximum energy spread. Although ϕ_m is lengthened in most cases, ΔE_M is smaller too.

2. For any distribution, when ϕ_m and ΔE_M are small, with fixed h , ω_0 , n and E ,

$$\Delta E_M \propto \phi_m \Omega_S \propto \phi_m V^{* \frac{1}{2}}. \quad (4.8)$$

Therefore,

$$N_C \left| \frac{Z}{n} \right|_{MW} \propto V^{* \frac{3}{2}} \phi_m^3. \quad (4.9)$$

But bunch area

$$S \propto \phi_m \Delta E_m \propto V^{* \frac{1}{2}} \phi_m^2 \quad (4.10)$$

giving

$$\phi_m \propto V^{* - \frac{1}{4}} \quad (4.11)$$

and

$$N_C \left| \frac{Z}{n} \right|_{MW} \propto V^{* \frac{1}{4}}. \quad (4.12)$$

Therefore, wall inductance will lower $N_c |Z/n|_{MW}$ although ϕ_m is increased in most cases.

3. From Eqs. (4.7 and (4.8), we get

$$N_c \left| \frac{Z}{n} \right|_{MW} \sim V^{*3/4} S^{3/2}. \quad (4.13)$$

We see from Figure 7 that this 3/2 power dependence on S is indeed correct when $|Z/n|_{ind} \rightarrow 0$ (or $r \rightarrow 0$).

4. In a previous note⁴, significant lower limits were obtained for microwave stability at zero wall impedance:

$$N_c \left| \frac{Z}{n} \right|_{MW} = \begin{cases} 0.68 \times 10^{11} \text{ ohms} & \text{at } 150 \text{ GeV}/c^2 \\ 1.6 \times 10^{11} \text{ ohms} & \text{at } 1000 \text{ GeV}/c^2. \end{cases}$$

There, a bi-Gaussian distribution in the longitudinal phase space was assumed instead of the elliptical distribution used here. The reason is, with bi-Gaussian distribution, $(\Delta E)_{FWHM}$ is smaller and I_{in} is bigger.

IV.2 When the beam current or the number of particles in a bunch exceeds the corresponding critical values for microwave stability, overshoots occur.

Dory's formula⁵ for overshoot gives

$$\left(\frac{\Delta E^2}{I_{in}} \right)_i \left(\frac{\Delta E^2}{I_{in}} \right)_f = \left(\frac{\Delta E^2}{I_{in}} \right)_c^2, \quad (4.14)$$

where the subscripts i and f denote before and after overshoot respectively, while the subscript c denotes critical. As overshoot takes place, the bunch length will change from ϕ_i to ϕ_f . Using elliptical distribution,

$$\left(\frac{(\Delta E)_{FWHM}^2}{I_{in}} \right)_j = \frac{3\beta^2 E e V^* (\phi_j) D_j}{\pi^2 |n| h I_{AV}}, \quad (4.15)$$

where j stands for i, f, or c. Therefore, Eq. (4.14) reduces to

$$\frac{V^*(\phi_i)D_i V^*(\phi_f)D_f}{I_{AV}^2} = \left(\frac{V^*(\phi_c)D_c}{I_c} \right)^2 \quad (4.16)$$

where the average total current is

$$I_{AV} = \frac{eNh\beta c}{2\pi R}, \quad (4.17)$$

the critical current is

$$I_c = \frac{eN_c h\beta c}{2\pi R}, \quad (4.18)$$

and D_j is given by

$$D_j = \sin \phi_j - \phi_j \cos \phi_j - \frac{k}{m} \left(\frac{\sin m\phi_j}{m} - \phi_j \cos m\phi_j \right). \quad (4.19)$$

In fact, when N is increased gradually to pass N_c , $\phi_i \rightarrow \phi_c$. Then, for a given beam energy and bunch area, the final overshoot bunch length can be found for a given number of particles per bunch. The results are plotted in Figures 8-13. Actually there is a maximum limit for N , because, as it increases, wall inductance will lower the effective RF voltage which has to be positive. Thus the bound of N is given by

$$1 - N \left| \frac{Z}{n} \right|_{MW} r \frac{e\beta c h^2}{2RV_{RF}D_c} \geq 0, \quad (4.20)$$

or

$$N \left| \frac{Z}{n} \right|_{MW} \leq \frac{2RV_{RF}D_c}{e\beta c h^2 r}. \quad (4.21)$$

For bunch area $S = 0.3$ eV-sec, $r = 5$, the following bounds are obtained:

Energy	ϕ_c	Bound for $N Z/n _{MW}$	
1000 GeV/c ²	0.45 rad	40x10 ¹⁰ ohms	(Landau on)
1000 GeV/c ²	0.44 rad	41x10 ¹⁰ ohms	(Landau off)
150 GeV/c ²	0.70 rad	170x10 ¹⁰ ohms	(Landau on)
150 GeV/c ²	0.72 rad	170x10 ¹⁰ ohms	(Landau off)

V. SINGLE BUNCH INSTABILITY

V.1 We have seen that Landau cavities introduce a large spread in the oscillation frequency within a bunch. Now we wish to make a quantitative estimate of the damping effect they do to single-bunch oscillations.

Our starting point is the unperturbed Hamiltonian (2.11)

$$H_0 = \frac{1}{2} a(\Delta E)^2 + \frac{\omega_0}{2\pi} U^*(q) . \quad (5.1)$$

Here we have replaced the RF phase variable ϕ of an orbit in the longitudinal phase space by q , and denote the maximum longitudinal displacement of the orbit by q_m , while reserving ϕ_m as the maximum of q_m or the longitudinal edge of the bunch, or the half length of the bunch. Thus $H_0 = \frac{\omega_0}{2\pi} U^*(q_m)$ for the particular orbit and $H_0 = \frac{\omega_0}{2\pi} U^*(\phi_m)$ for the outermost orbit. It will be convenient to change to action-angle variables J and θ defined by

$$\begin{aligned} J &= \oint \Delta E(q) dq \\ &= 4 \left(\frac{\beta^2 E e V^*}{\pi |n| h} \right)^{\frac{1}{2}} \int_0^{q_m} dq \left[\cos q - \cos q_m - \frac{k}{m} (\cos m q - \cos m q_m) \right]^{\frac{1}{2}} \end{aligned} \quad (5.2)$$

and

$$\dot{\theta} = \frac{\partial H_0}{\partial J} = \frac{\Omega_s(J)}{2\pi} \quad (5.3)$$

with $\Omega_s(J)$ given by Eq. (2.15).

V.2 To study instability, we need to solve a Vlasov equation,

$$\frac{\partial \psi}{\partial t} + \frac{\partial H}{\partial J} \frac{\partial \psi}{\partial \theta} - \frac{\partial H}{\partial \theta} \frac{\partial \psi}{\partial J} = 0, \quad (5.4)$$

where

$$\psi(J, \theta) = \psi_0(J, \theta) + \psi_1(H, \theta) e^{-i\Omega t} \quad (5.5)$$

the distribution of the bunch particles in the longitudinal phase space has a small perturbing part ψ_1 , oscillating with a coherent frequency Ω , which in turn introduces a perturbing part of the same frequency in the Hamiltonian

$$H(J, \theta) = H_0(J) + H_1(J, \theta) e^{-i\Omega t}. \quad (5.6)$$

Since ψ_0 is time-independent, the zeroth order of Eq. (5.4) says ψ_0 is a function of J only. The first order gives

$$-i\Omega \psi_1 + \frac{\partial H_0}{\partial J} \frac{\partial \psi_1}{\partial \theta} - \frac{\partial \psi_0}{\partial J} \frac{\partial H_1}{\partial \theta} = 0 \quad (5.7)$$

with $\partial H_0 / \partial J = \Omega_s / 2\pi$.

Since $\psi_1(J, \theta)$ is periodic in θ , we can write

$$\psi_1(J, \theta) = \sum_p R_p(J) e^{i2\pi p \theta}. \quad (5.8)$$

Substituting it in Eq. (5.7) leads to

$$\left[\Omega - p\Omega_s(J) \right] R_p(J) = -2\pi p \frac{d\psi_0}{dJ} \int_0^1 d\theta H_1(J, \theta) e^{-i2\pi p \theta} \quad (5.9)$$

where the periodicity of H_1 in θ has been used.

V.3 The perturbing Hamiltonian is given by

$$H_1 = ie\beta c I_{AV} \sum_n \lambda_1(q); \quad (5.10)$$

(for completeness, a proof is given in the Appendix). The perturbing line density $\lambda_1(q)$ has the same coherent frequency

$$\lambda = \lambda_0 + \lambda_1 e^{-i\Omega t}, \quad (5.11)$$

and is related to ψ_1 , by

$$\lambda_1(q) = \int \psi_1(\Delta E, q) \frac{R}{h} d \Delta E. \quad (5.12)$$

The rigid dipole mode is the mode that can be excited most easily and is also the most unstable mode. For this reason, we shall devote the rest of this discussion to this mode only. By definition, for the rigid dipole mode,

$$\lambda_1(q) = \frac{d\lambda_0}{dq} \bar{q} = \int R_1(J) e^{2\pi i \theta} d \Delta E, \quad (5.13)$$

where from

$$\int q \lambda_1 dq = \bar{q} \int q \frac{d\lambda_0}{dq} dq = -\bar{q} \frac{h}{R}, \quad (5.14)$$

\bar{q} can be deduced,

$$\bar{q} = -\frac{R}{h} \int q R_1(J) e^{2\pi i \theta} d \Delta E dq. \quad (5.15)$$

The RF phase q , being periodic in $\alpha = 2\pi\theta$, can be Fourier expanded

$$q = \sum_{n=1,2,\dots} \tilde{q}_{2n+1}(J) \cos(2n+1)\alpha, \quad (5.16)$$

thus giving

$$\bar{q} = -\frac{R}{2h} \int dJ \tilde{q}_1(J) R(J). \quad (5.17)$$

In obtaining Eq. (5.16), we have set $q = q_m$ at $\theta = 0$; then q will vanish at $\alpha = (2n+1)\pi/2$. As a result, only odd harmonics appear in Eq. (5.16).

Using Eqs. (2.9), (5.13), (5.17) and (5.10), the Vlasov equation becomes

$$\begin{aligned} \left[\Omega - \Omega_S(J) \right] R_1(J) = & -i \frac{\pi e \beta c}{2D_m} I_{AV} \frac{Z}{n} \frac{d\psi_0}{dJ} \int dJ' \tilde{q}_1(J') R_1(J') \\ & \cdot \int_0^1 d\theta e^{-2\pi i \theta} (-\sin q + k \sin m q). \end{aligned} \quad (5.18)$$

As will be shown below that, in the expansion of q in Eq. (5.16), only the first term dominates, we can therefore retain only the first term. Then the last integral in Eq. (5.18) can be done neatly to give

$$-J_1(\tilde{q}_1) + k J_1(m\tilde{q}_1)$$

where J_1 is the Bessel function of order 1. In Eq. (5.18), we note that the integral

$$\int dJ' \tilde{q}_1(J') R_1(J') \quad (5.19)$$

is a constant independent of J . Thus we can eliminate R_1 and arrive at the dispersion relation

$$1 = i \frac{Z}{n} \frac{\pi e \beta c}{2D_m} I_{AV} \int dJ \frac{\tilde{q}_1 \frac{d\psi_0}{dJ} \left[J_1(\tilde{q}_1) - J_1(m\tilde{q}_1) \right]}{\Omega - \Omega_S(J)}, \quad (5.20)$$

or, using q_m as the dummy variable instead,

$$1 = i \frac{Z}{n} \frac{\pi e \beta c}{2D_m} I_{AV} \int_0^{\phi_m} dq_m \frac{\tilde{q}_1 \frac{d\psi_0}{dq_m} \left[J_1(\tilde{q}_1) - k J_1(m\tilde{q}_1) \right]}{\Omega - \Omega_S(q_m)}. \quad (5.21)$$

V.4 The next task is to compute \tilde{q}_1 as a function of q_m or J . We have

$$\frac{dq}{dt} = 2\pi \left(\frac{\partial q}{\partial \alpha} \frac{\partial H}{\partial J} - \frac{\partial q}{\partial J} \frac{\partial H}{\partial \alpha} \right), \quad (5.22)$$

since H_0 is α -independent. From Eq. (5.10), we know that H_1 is a function of q only; so using Eqs. (5.22) and (5.3),

$$\begin{aligned}
 \frac{dq}{dt} &= 2\pi \frac{\partial q}{\partial \alpha} \left(\frac{\partial H}{\partial J} - \frac{\partial q}{\partial J} \frac{\partial H_1}{\partial q} \right) \\
 &= 2\pi \frac{\partial q}{\partial \alpha} \left(\frac{\partial H}{\partial J} - \frac{\partial H_1}{\partial J} \right) \\
 &= 2\pi \frac{\partial q}{\partial \alpha} \frac{\partial H_0}{\partial J} \\
 &= \Omega_s(J) \frac{\partial q}{\partial \alpha}, \tag{5.23}
 \end{aligned}$$

where $\Omega_s(J)$ is given by Eq. (2.15). From the Hamiltonian (5.6), we also get

$$\frac{dq}{dt} = \frac{\partial H}{\partial p} = \left\{ \frac{a\omega_0}{\pi} \left[U^*(q_m) - U^*(q) \right] \right\}^{\frac{1}{2}}. \tag{5.24}$$

Combining Eqs. (5.23) and (5.24), α can be reduced as a function of q :

$$\begin{aligned}
 \alpha &= - \frac{\Omega_s(q_m)}{\Omega_{s0}} \int_{q_m}^q dq' \left\{ 2 \left[\cos q' - \cos q_m - \frac{k}{m} (\cos mq' - \cos mq_m) \right] \right\}^{\frac{1}{2}} \\
 &\equiv f(q). \tag{5.25}
 \end{aligned}$$

From Eq. (5.16), we get

$$\tilde{q}_{2n+1}(J) = \frac{4}{\pi} \int_0^{\pi/2} q(J, \alpha) \cos(2n+1)\alpha \, d\alpha. \tag{5.26}$$

Substituting Eq. (5.25) in Eq. (5.26) and changing the variable of interaction to q , we arrive at

$$\tilde{q}_{2n+1}(q_m) = \frac{4}{\pi} \int_0^{q_m} q f'(q) \cos[(2n+1)f(q)] \, dq. \tag{5.27}$$

When q_m is small the Fourier expansion of q in Eq. (5.16) can be computed exactly as

$$\tilde{q}_{2n+1} = q_m \frac{2\sqrt{2}\pi}{K(\frac{1}{2})} \frac{e^{-(n+\frac{1}{2})\pi}}{1+e^{-(2n+1)\pi}}. \tag{5.28}$$

Equation (5.27) has been computed numerically. The results, together with

those in Eq. (5.28) are listed in Table I. We see that when the Landau cavities are turned off \tilde{q}_1/q_m deviates from unity by less than 0.15% for half bunch length ≤ 0.5 rad. When the Landau cavities are turned on, \tilde{q}_1/q_m deviates from unity by less than 5%.

V.5 Now we are going to solve the dispersion relation (5.21).

The elliptical distribution (2.8), after normalization to unity, becomes

$$\psi_0 = \frac{h}{RD_m} \left(\frac{|n|h}{\pi B^2 E e V^*} \right)^{\frac{1}{2}} \left[\cos q_m - \cos \phi_m - \frac{k}{m} (\cos m q_m - \cos m \phi_m) \right]^{\frac{1}{2}} \quad (5.29)$$

which is a function of q_m only. Substituting in Eq. (5.21), the dispersion relation becomes

$$iN \frac{Z}{n} = \frac{4RV_{RF}}{eBch^2} \left(\frac{V^*}{V} \right)^{\frac{1}{2}} D_m^2 I^{-1} \quad (5.30)$$

and the dispersion integral is

$$I = \int_0^{\phi_m} dq_m \frac{\tilde{q}_1 (\sin q_m - k \sin m q_m) |J_1(\tilde{q}_1) - k J_1(m\tilde{q}_1)|}{\left[\bar{\Omega} - \bar{\Omega}_s(q_m) \right] 2^{\frac{1}{2}} \left[\cos q_m - \cos \phi_m - \frac{k}{m} (\cos m q_m - \cos m \phi_m) \right]^{\frac{1}{2}}}, \quad (5.31)$$

where the normalized coherent frequency $\bar{\Omega}$ and the normalized synchrotron frequency $\bar{\Omega}_s(q_m)$ are defined as

$$\bar{\Omega} = \Omega / \Omega_{s0}$$

$$\bar{\Omega}_s(q_m) = \Omega_s(q_m) / \Omega_{s0} \quad (5.32)$$

Equation (5.30) can now be solved for the stability limit. Care must be taken that V^*/V given by Eq. (2.13) depends on the inductive part of NZ/n . The results are plotted as solid curves in Figure 14 when the Landau cavities are off and in Figure 15 when the cavities are on.

V.6 Remarks

(1) The stability area enclosed by the stability curve is more than an order of magnitude bigger when the Landau cavities are turned on. This is obviously due to the extra spread of the synchrotron frequency introduced by the Landau cavities.

(2) The stability curves at extraction energy encloses less area than the curves at injection energy. This is because at extraction energy, the bunch length is very much shorter. The frequency spread is therefore small, so lessening Landau damping.

(3) The impedance per harmonic in the RF region is $Z/n \sim 5(1-i)\Omega$ for both injection and extraction energies (negative imaginary part is inductive). Thus for a 2×10^{10} bunch, the rigid dipole mode is definitely unstable without the Landau cavities. However, with the Landau cavities turned on, the stability curves do not extend into the inductive region at all. The reason is that, the elliptical distribution which we have assumed, has infinite slope at the bunch edge. This singular point forces that stability curves to $NZ/n = 0$ rather abruptly.

Since $d\Omega_s(q_m)/dq_m$ is negative without Landau cavities and positive with Landau cavities, the stability curves for the former situation extend into the inductive region only while those for the latter situation extend into the capacitive region only.

(4) In order to avoid the singular point introduced by the elliptical distribution at $q_m = \phi_m$, we try a distribution

$$\psi_0 \propto \left[\Delta E(q)_M^2 - \Delta E^2 \right]^2 \quad (5.33)$$

which behaves like $\sim (\phi_m^2 - q_m^2)^2$ for small ϕ_m and has continuous derivative at the bunch edge. The stability curves are also plotted in Figures 14 and 15 as dashed curves. Because there is no singular point, the stability curves extend

into both the inductive and capacitive regions in all cases. We see that for $NZ/n \sim 10(1-i) \times 10^{10}$ ohms, the rigid dipole mode is definitely stable at injection energy when the Landau cavities are turned on, but is only on the edge of stability at extraction energy. An estimate of the critical $|NZ/n|$ will be given in the next section.

The switching of distribution from elliptical to Eq. (5.33) at this moment will make our discussion inconsistent because the voltage reduction of Eq. (2.13) was formulated with elliptical distribution. However, such a computation will still remain meaningful if, by changing the distribution, the voltage reduction is not affected too much. This may be our case because the voltage reduction is not big anyway.

We believe that, starting from the elliptical distribution, the bunch is unstable against dipole oscillation because the bunch edge has infinite gradient. The bunch edge will grow so lessening the gradient until it becomes stable. In other words, the distribution will adjust itself so that the gradient at the edge is smoothed out to such an extent that the bunch becomes stable.

VI VARIATION OF M IN LANDAU CAVITY

In this section, we vary m but keeping $km = 1$ and investigate the effect of the Landau cavities on bunch length, microwave stability and single bunch stability.

(1) Bunch length

With the Landau cavities turned on, the RF potential is

$$U \propto -V_{RF} \left(\cos \phi - \frac{1}{m^2} \cos m\phi \right) + \text{constant} \quad (6.1)$$

which, when ϕ is small, becomes

$$U \propto \frac{m^2 - 1}{24} V_{RF} \phi^4 \quad (6.2)$$

Thus reducing m implies reducing the RF voltage, which becomes zero when

$m \rightarrow 1$. Thus with a fixed bunch area, bunch length will increase and reach infinity when $m \rightarrow 1$. This is illustrated in Figure 16 where the limitation of small bunch length has been relaxed.

(2) Critical microwave stability limit

When the bunch length ϕ_m is small, the maximum instantaneous current is inversely proportional to ϕ_m . Thus, according to Eq. (4.1),

$$N_c \left| \frac{Z}{n} \right|_{MW} \propto \frac{(\Delta E)_{FWHM}^2}{E} \cdot \phi_m$$

$$\sim \left(\frac{\Delta E}{E} \right)_{FWHM} S, \quad (6.3)$$

where S is the bunch area. As m decreases, ϕ_m increases. Thus, keeping S fixed, $(\Delta E)_{FWHM}$ will decrease and therefore $N_c \left| \frac{Z}{n} \right|_{MW}$ will be decreased also.

(3) Single bunch stability

By numerical computation, the stability curves for $m = 4$ and distribution (5.33) are plotted dash-dotted in Figure 15. We see that, at injection energy of $150 \text{ GeV}/c^2$, the curve encloses a much bigger area than the $m = 9$ curve. But at extraction energy of $1000 \text{ GeV}/c^2$, the $m = 4$ curve does not differ very much from the $m = 9$ curve. In order to understand this, we make the following analysis and derive a formula for the critical $N_c \left| \frac{Z}{n} \right|_{ind}$.

The stability curves depend on two factors: (a) bunch length ϕ_m , the bigger the bunch length the bigger the frequency spread, and (b) $d\Omega_s/dq_m$, the rate of spread of the synchrotron frequency. Both factors depend on m .

In all our cases $\phi_m < 1$. Thus we can try a small ϕ_m approximation. (In fact, ϕ is multiplied by m in the argument of sine or cosine in Eq.(6.1) for example; thus an expansion in ϕ_m may not be justified.) Using the distribution (5.33), the dispersion relation is

$$iN \frac{Z}{n} = \frac{16 C_m D_m}{15 \pi} \frac{RV_{RF}}{e\beta c h^2} \left(\frac{V^*(\phi_m)}{V_{RF}} \right)^{\frac{1}{2}} I^{-1} \quad (6.4)$$

where

$$I = \int_0^{\phi_m} dq_m 2\tilde{q}_1 \left[\sin q_m - k \sin m q_m \right] \left[J_1(\tilde{q}_1) - k J_1(m\tilde{q}_1) \right] \\ \cdot \left[\cos q_m - \cos \phi_m - \frac{k}{m} (\cos m q_m - \cos m \phi_m) \right] \left[\bar{\Omega} - \bar{\Omega}'_s(q_m) \right]^{-1} \quad (6.5)$$

and C_m is some normalization factor of the distribution (5.33). We are interested in the point where the stability curve crosses the $\text{Re}(NZ/n)$ axis. This is in fact the point $q_m = \phi_m$. So we can expand the numerator of Eq. (6.5) around $q_m = 0$ and the denominator around $q_m = \phi_m$ yielding.

$$I = - \frac{s^4 (m^2 - 1)^3 \phi_m^{11}}{1152 \bar{\Omega}'_s(\phi_m)} \int_0^1 dx \frac{x^7 (1-x^4)}{1-x} \quad (6.5)$$

where s is defined by

$$\tilde{q}_1 \approx s q_m$$

and is given by Eq. (5.28)

$$s = \frac{2\sqrt{2} \pi}{K(\frac{1}{2})} \frac{e^{-\pi/2}}{1+e^{-\pi}} = .955 . \quad (6.6)$$

When ϕ_m is small, the two normalization factors give

$$D_m \rightarrow \frac{m^2 - 1}{30} \phi_m^5 , \\ C_m \rightarrow \left(\frac{m^2 - 1}{12} \right)^{5/2} \phi_m^{11} \int_0^1 dx (1-x^4)^{5/2} . \quad (6.7)$$

Putting Eqs. (6.5), (6.6), (6.7) in Eq. (6.4), we arrive at

$$\left| \frac{NZ}{n} \right|_c = 182 \left(\frac{V^*}{V_{RF}} \right)^{\frac{1}{2}} (m^2 - 1)^{\frac{1}{2}} \phi_m^5 \bar{\Omega}'_s(\phi_m) \quad (6.8)$$

in 10^{10} ohms. This formula gives rather good estimates of the critical NZ/n as shown in Table II.

We note that Eq. (6.8) depends on the deviations of the synchrotron frequency at the bunch edge. From Figure 17, we see that the slope for the $m=4$ synchrotron frequency curve does not change much when the particle energy changes from $1000 \text{ GeV}/c^2$ to $150 \text{ GeV}/c^2$, whereas the change is very large for the $m=9$ curve, which has nearly zero slope at $150 \text{ GeV}/c^2$. This explains why at $150 \text{ GeV}/c^2$ the $m=9$ stability curve in Figure 15 crosses the real NZ/n axis at a much smaller value than the $m=4$ curve. In Reference 2, Sacherer made his analysis with small phase angle approximation from the beginning. He approximated the denominator of the dispersion integral (one similar to our Eq. (6.5)) by expanding $\bar{\omega}_s$ around $q_m = 0$ instead. There, $\bar{\omega}'_s \propto (m^2-1)^{1/2}$ and his formula for critical NZ/n is

$$\left| \frac{NZ}{n} \right| \propto (m^2-1) \phi_m^5 \quad (6.9)$$

which does not agree with the results from numerical computation. (See last column of Table II.)

When the Landau cavities are turned off, a small angle formula for critical NZ/n can also be obtained:

$$\left| \frac{NZ}{n} \right|_c = 984 (V^*/V_{RF})^{1/2} \phi_m^4 \left| \bar{\omega}'_s(\phi_m) \right| \quad (6.10)$$

in 10^{10} ohms. However $\bar{\omega}'_s$ does not change much for ϕ_m up to unity, and it does matter whether $\bar{\omega}'_s$ is computed at $q_m = 0$ or ϕ_m . Using the expansion of Eq. (1.1), we get

$$\left| \frac{NZ}{n} \right|_c = 123 (V^*/V_{RF})^{1/2} \phi_m^5 (10^{10} \text{ ohms}) . \quad (6.11)$$

The results are tabulated in Table III. They agree with the numerically computed results quite well.

References

1. F. Sacherer, Proc. 1973 Part. Accel. Conf., San Francisco, IEEE Trans. on Nucl. Sci., Vol. NS-20, No. 3, p. 825
2. S. Ohnuma, Fermilab TM-749
3. F. Sacherer, "Longitudinal Stability with a Landau Cavity", National Synchrotron Light Source Project Workshop, June 1977
4. K. Ng, Fermilab UPC-150
5. R.A. Dory, MURA Report No. 654 (1962)

TABLE I

CAVITY	QM	OMEGA	Q1/QM	Q3/QM	Q5/QM
ON	.00000	.00000	.95501	.04305	.00186
ON	.05000	.15405	.95524	.04287	.00181
ON	.10000	.30436	.95600	.04239	.00165
ON	.15000	.44741	.95714	.04143	.00138
ON	.20000	.57982	.95883	.04017	.00101
ON	.25000	.69873	.96105	.03846	.00054
ON	.30000	.80175	.96382	.03628	-.00004
ON	.35000	.88712	.96718	.03360	-.00070
ON	.40000	.95378	.97116	.03034	-.00144
ON	.45000	1.00142	.97578	.02647	-.00224
ON	.50000	1.03056	.98102	.02192	-.00304
ON	.55000	1.04254	.98683	.01670	-.00379
ON	.60000	1.03958	.99307	.01087	-.00440
ON	.65000	1.02472	.99946	.00460	-.00479
ON	.70000	1.00180	1.00558	-.00174	-.00483
ON	.75000	.97520	1.01082	-.00760	-.00447
ON	.80000	.94940	1.01454	-.01225	-.00369
ON	.85000	.92820	1.01619	-.01508	-.00259
ON	.90000	.91401	1.01565	-.01577	-.00132
ON	.95000	.90735	1.01328	-.01452	-.00007
ON	1.00000	.90716	1.00982	-.01194	.00103

CAVITY	QM	OMEGA	Q1/QM	Q3/QM	Q5/QM
OFF	.00000	1.00000	1.00000	-.00000	-.00000
OFF	.05000	.99984	1.00001	-.00001	-.00000
OFF	.10000	.99938	1.00005	-.00005	-.00000
OFF	.15000	.99859	1.00012	-.00012	.00000
OFF	.20000	.99750	1.00021	-.00021	.00000
OFF	.25000	.99610	1.00033	-.00033	.00000
OFF	.30000	.99438	1.00047	-.00047	.00000
OFF	.35000	.99235	1.00064	-.00064	.00000
OFF	.40000	.99001	1.00084	-.00084	.00000
OFF	.45000	.98736	1.00107	-.00107	.00000
OFF	.50000	.98439	1.00132	-.00132	.00000
OFF	.55000	.98112	1.00160	-.00161	.00000
OFF	.60000	.97754	1.00191	-.00192	.00001
OFF	.65000	.97365	1.00225	-.00226	.00001
OFF	.70000	.96945	1.00262	-.00263	.00001
OFF	.75000	.96494	1.00302	-.00304	.00002
OFF	.80000	.96012	1.00345	-.00347	.00002
OFF	.85000	.95500	1.00391	-.00394	.00003
OFF	.90000	.94957	1.00441	-.00445	.00003
OFF	.95000	.94383	1.00494	-.00498	.00004
OFF	1.00000	.93779	1.00550	-.00556	.00005

Table II

m	Energy in GeV/c ²	ϕ_m in rad	$\bar{\omega}'_s(\phi_m)$	$ NZ/n _c$ in 10 ¹⁰ ohms		
				Eq. (6-8)*	Fig. 15	Sacherer*
4	1000	.453	1.08	14.5	12.5	18.0
4	150	.632	.86	60.9	53.8	94.8
9	1000	.351	1.45	12.5	12.5	26.7
9	150	.509	.38	21.2	24.5	173

Assuming $V^ = V_{RF}$

Table III

Energy in GeV/c ²	in rad	$ NZ/n _c$ in 10 ¹⁰ ohms	
		Eq. (6-11)*	Fig. 14
1000	.311	.358	.31
150	.503	3.96	3.15

Assuming $V^ = V_{RF}$

Figure 1

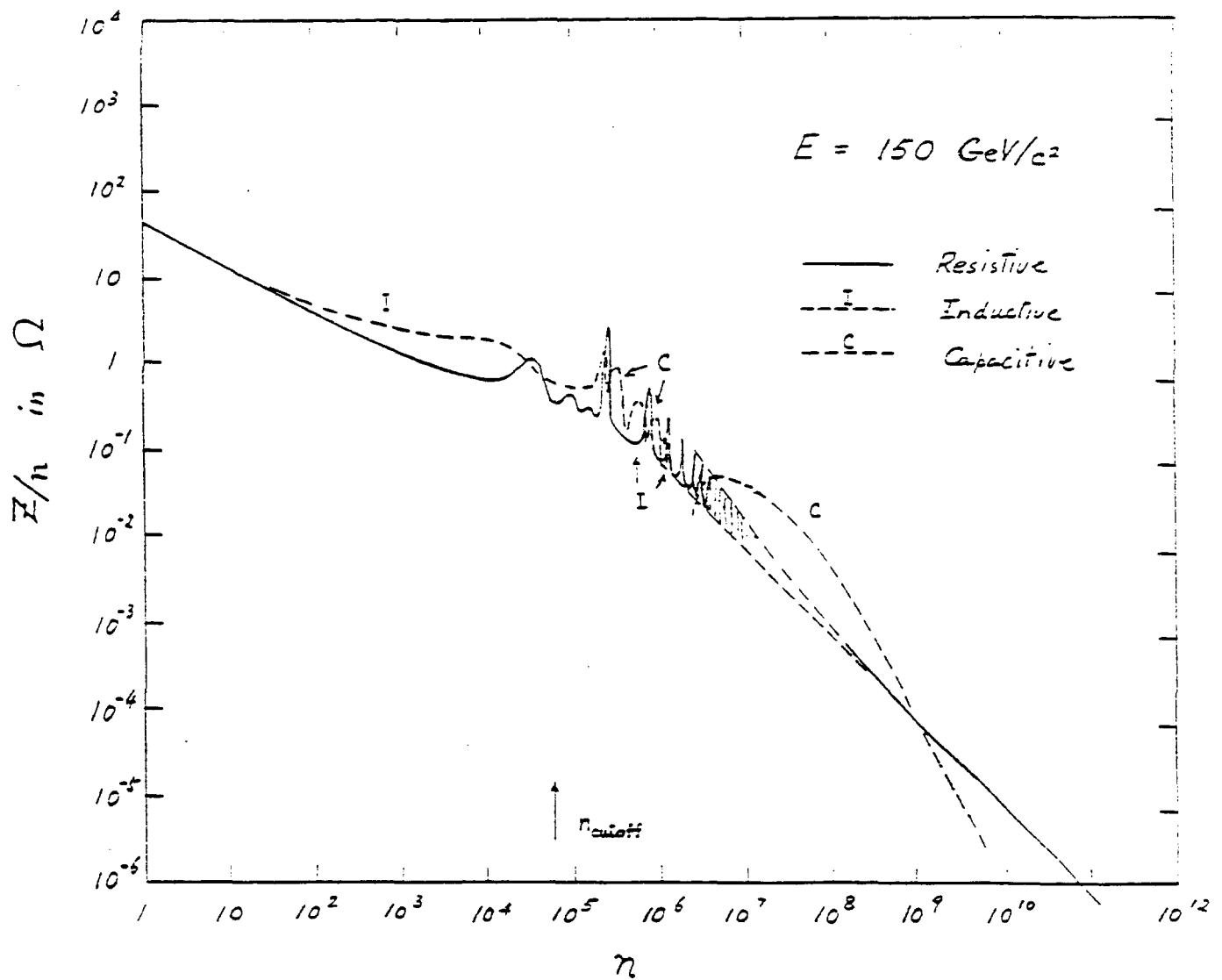


Figure 2

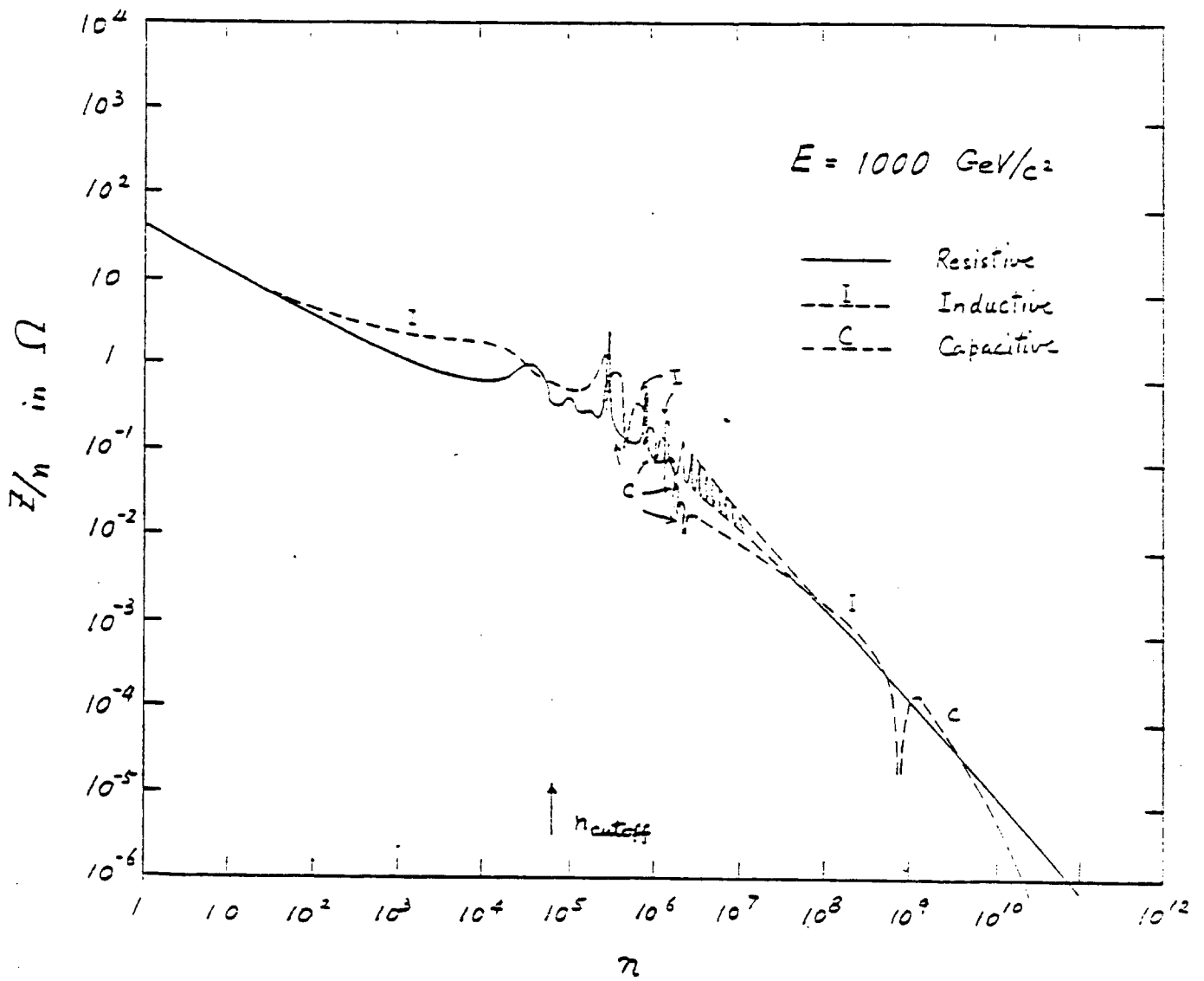


Figure 3

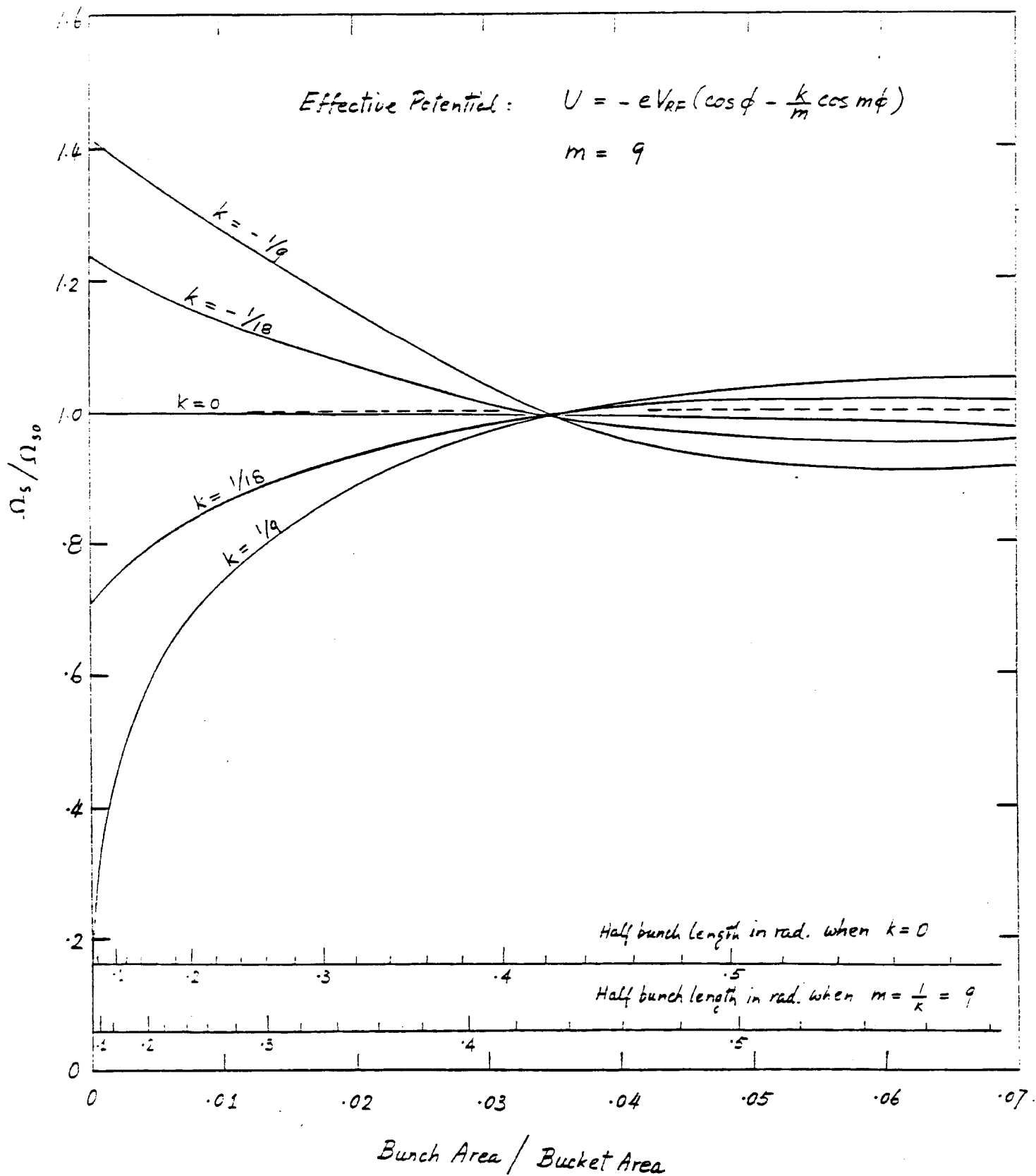


Figure 4

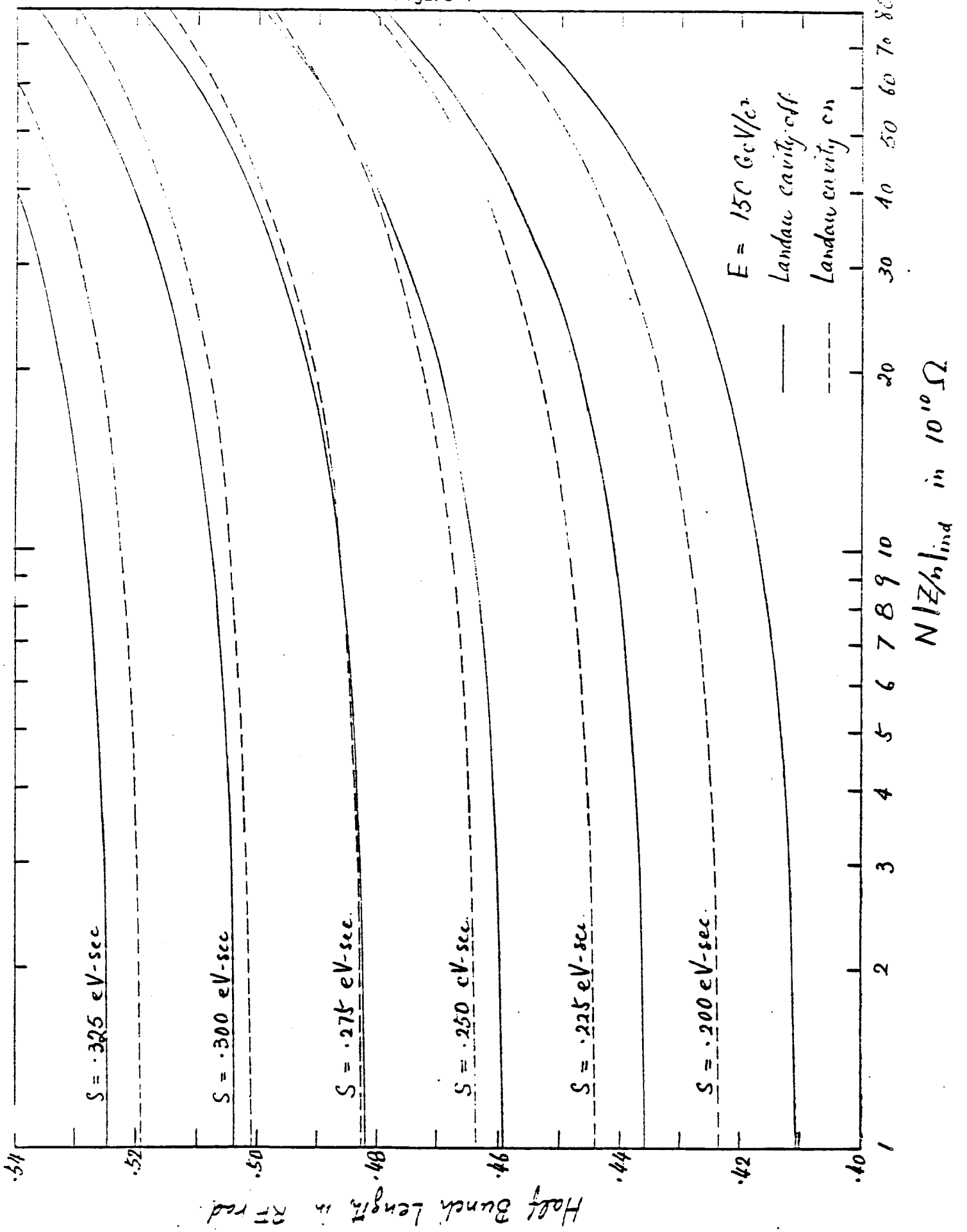


Figure 5

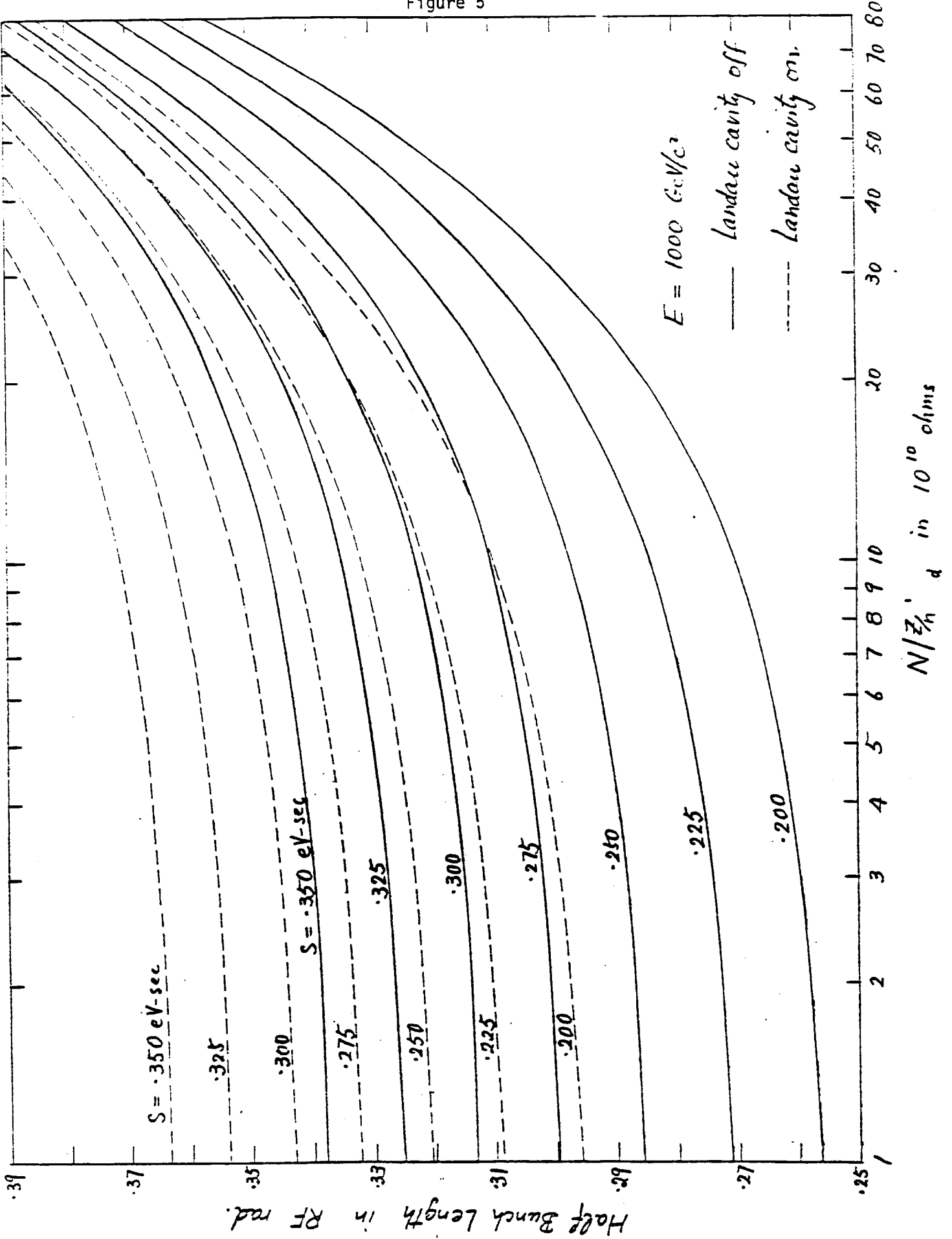


Figure 6

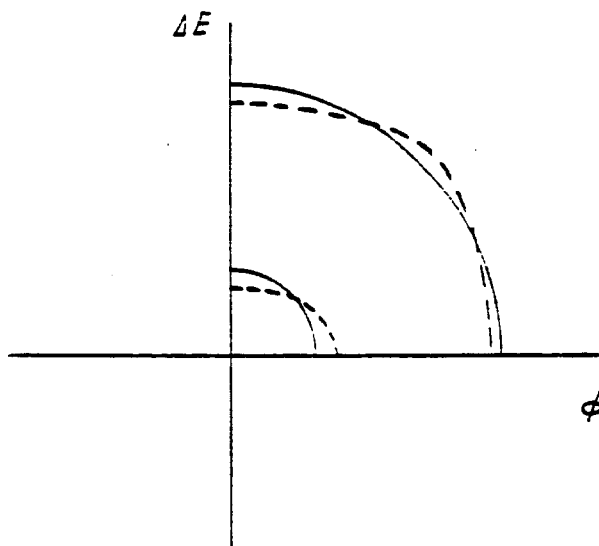
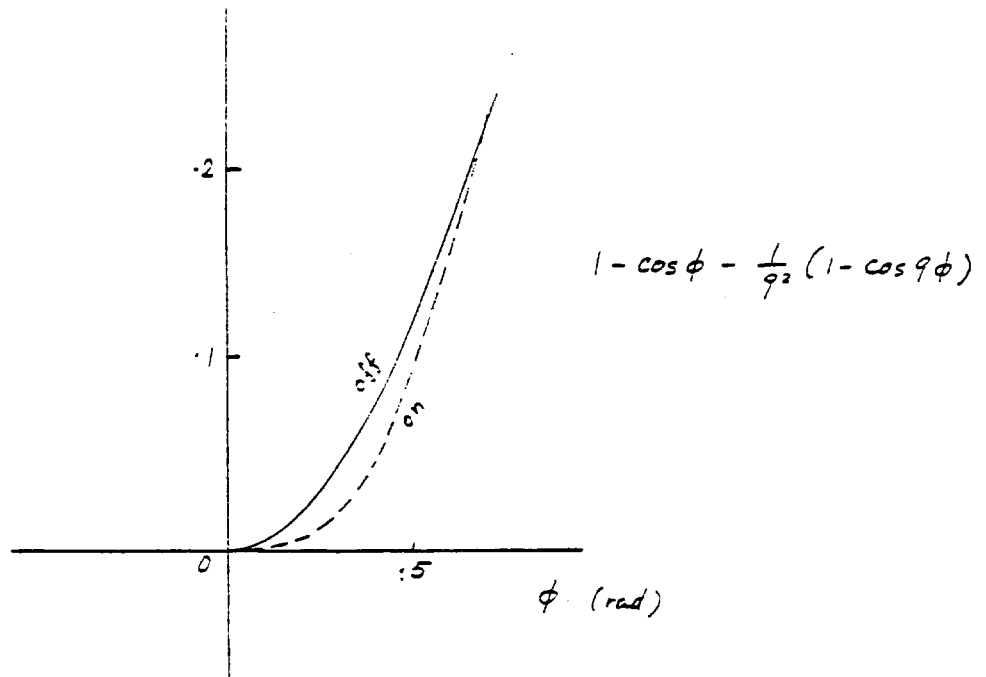
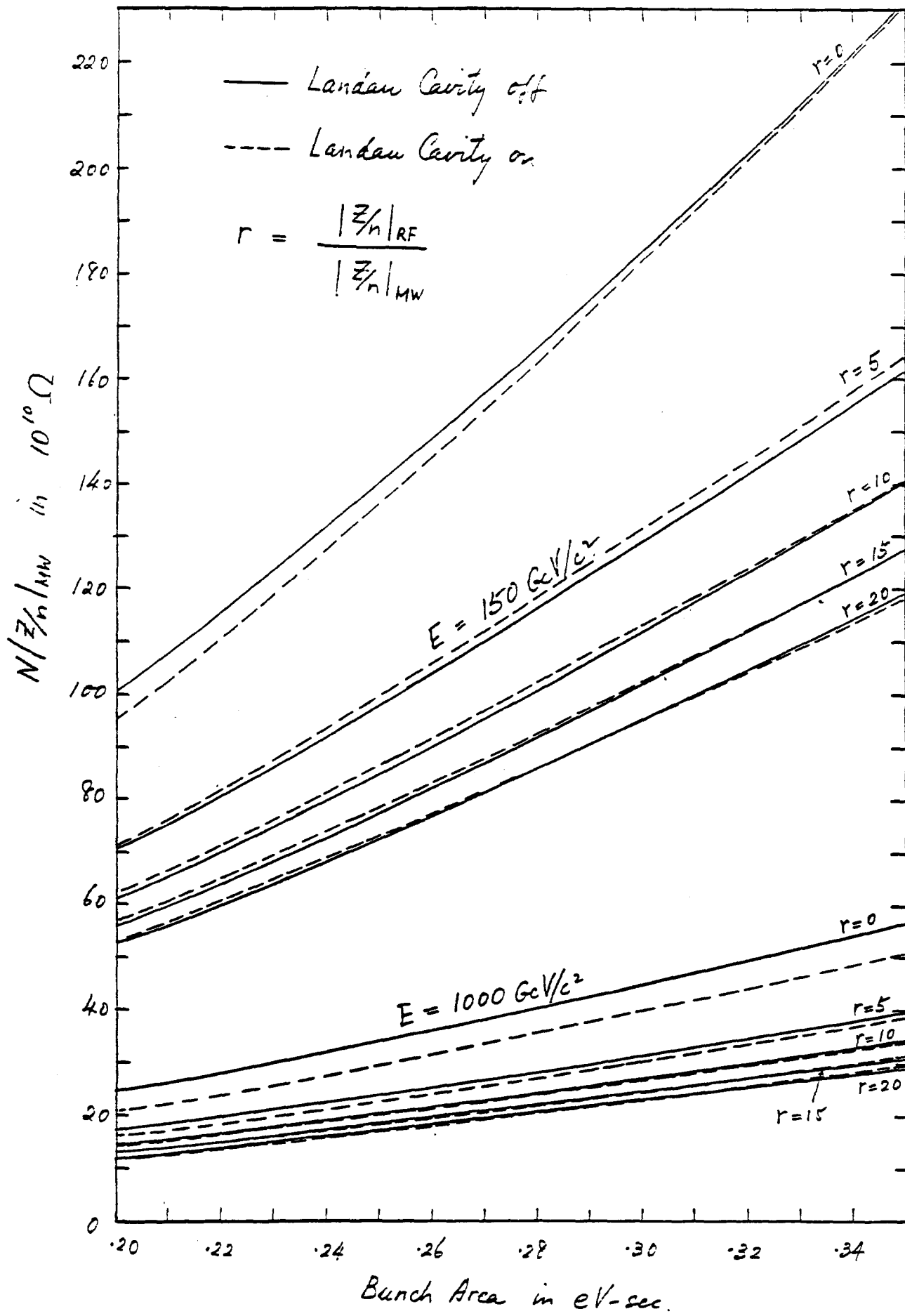


Figure 7



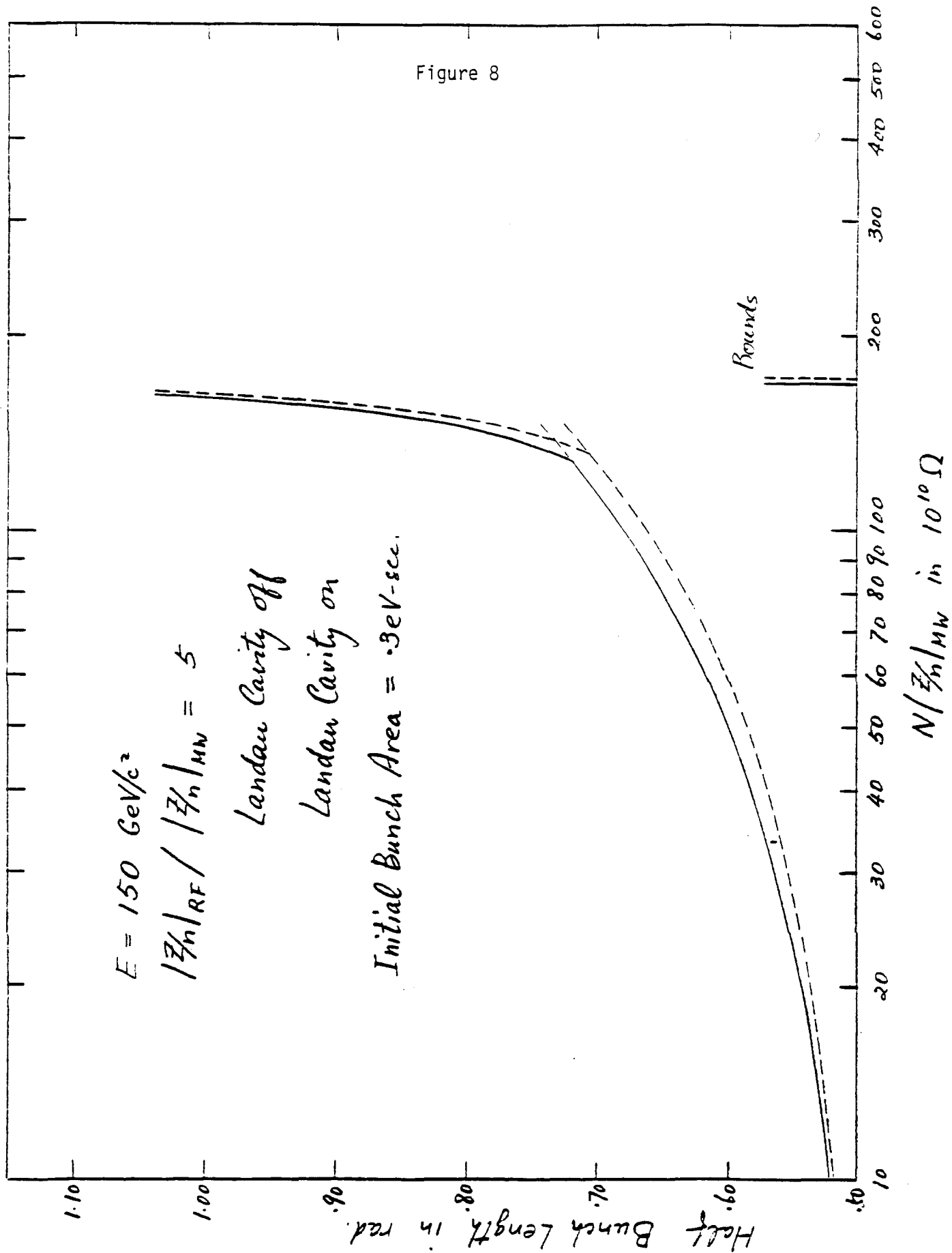


Figure 9

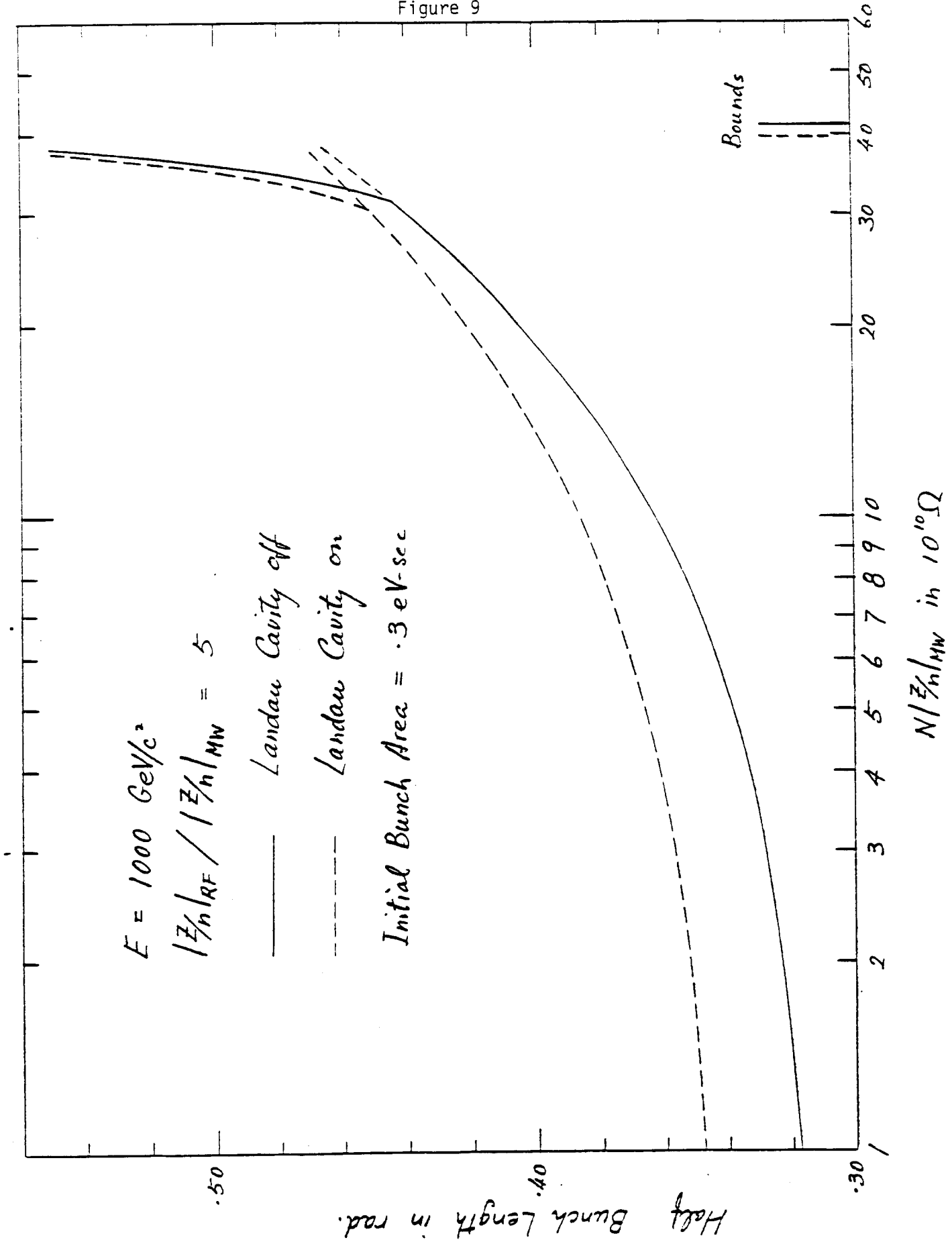


Figure 10

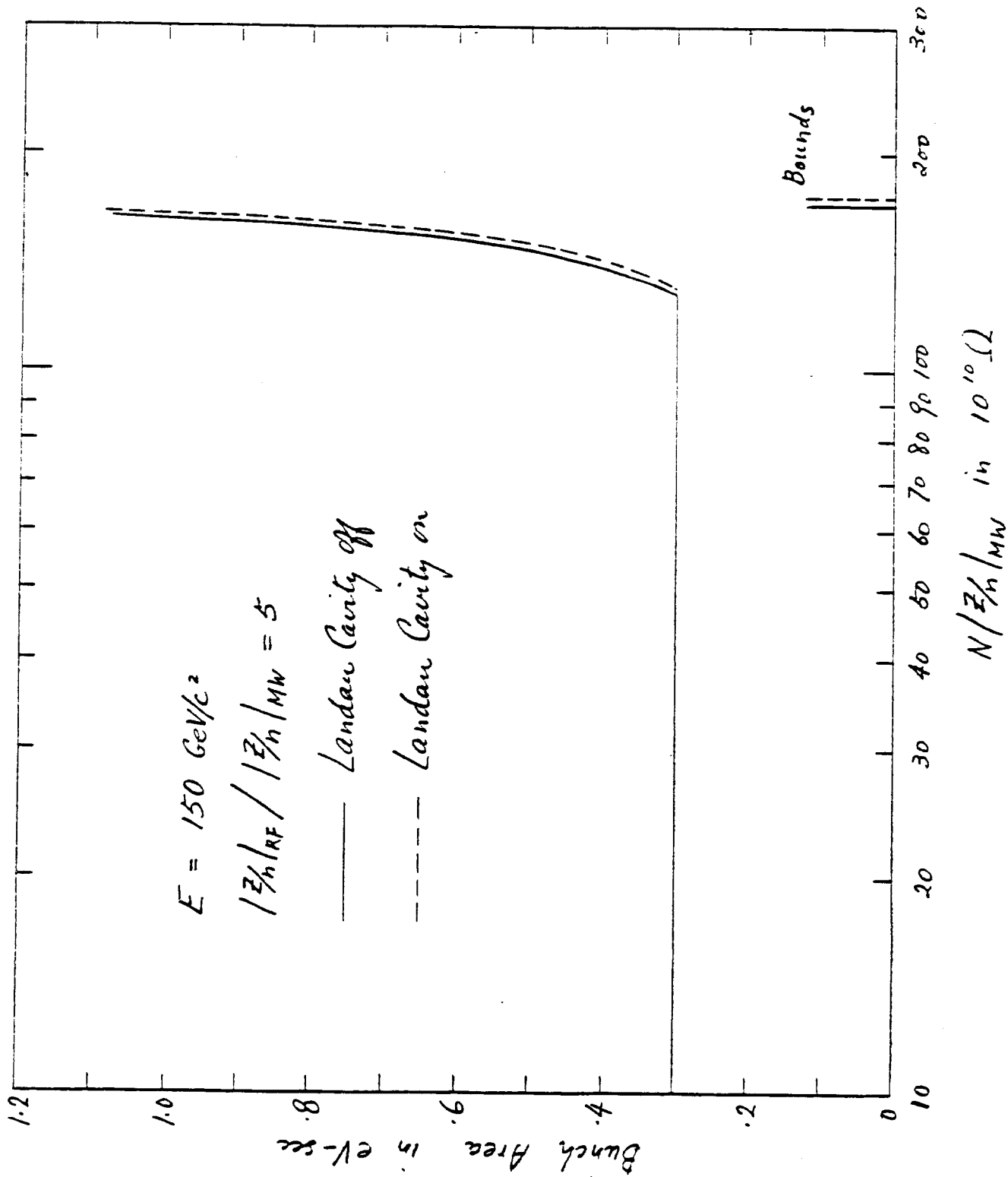


Figure 11

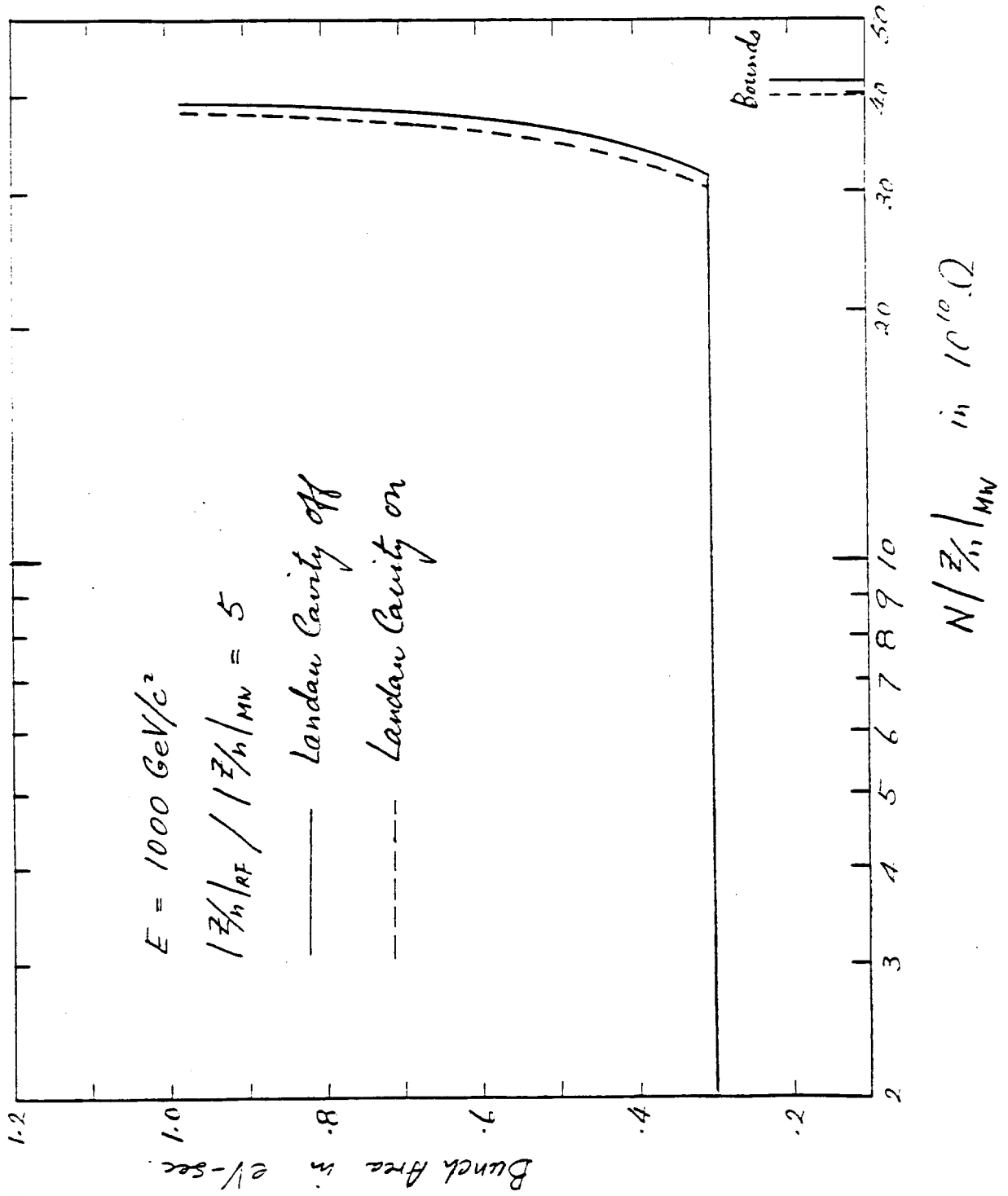


Figure 12

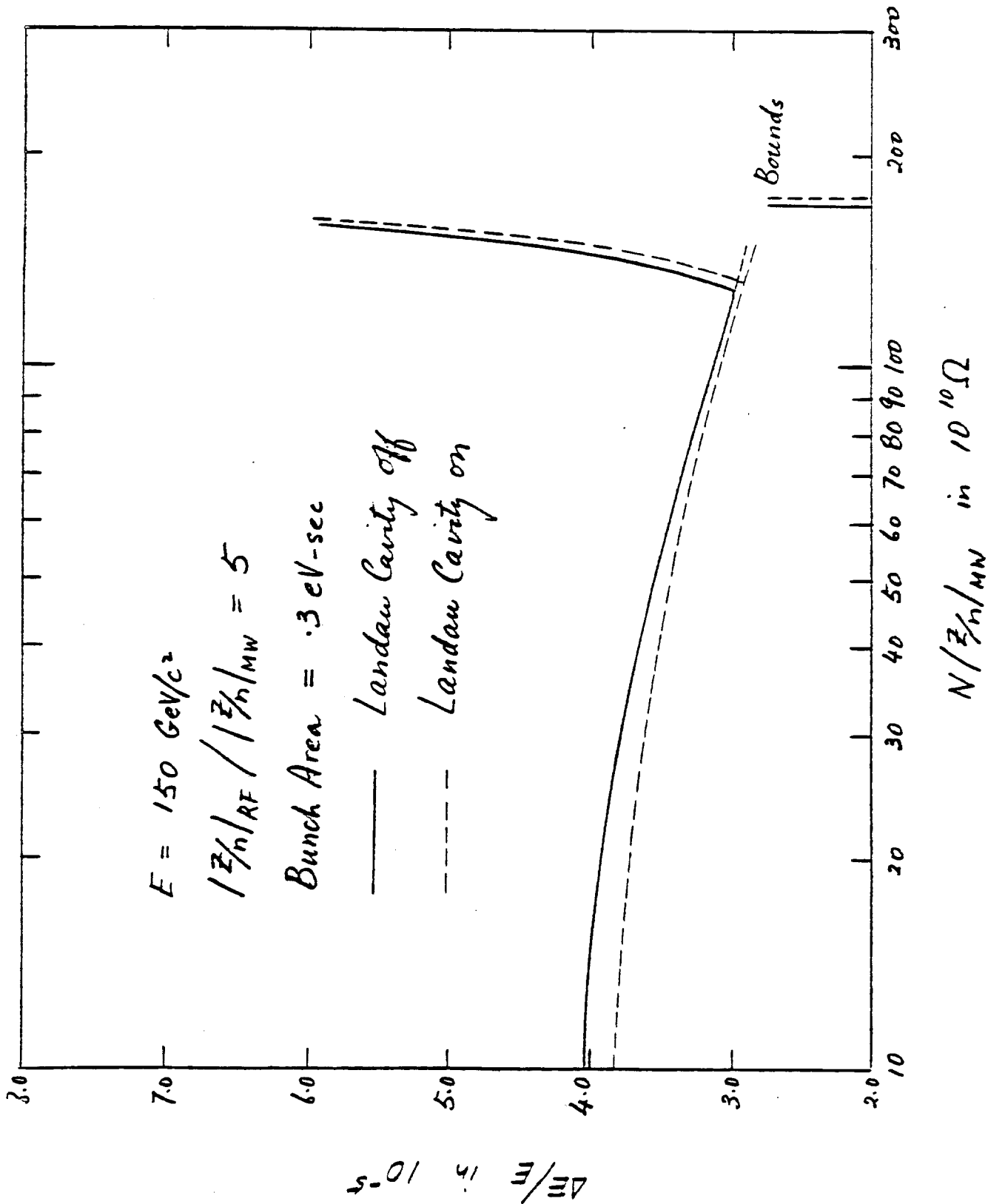


Figure 13

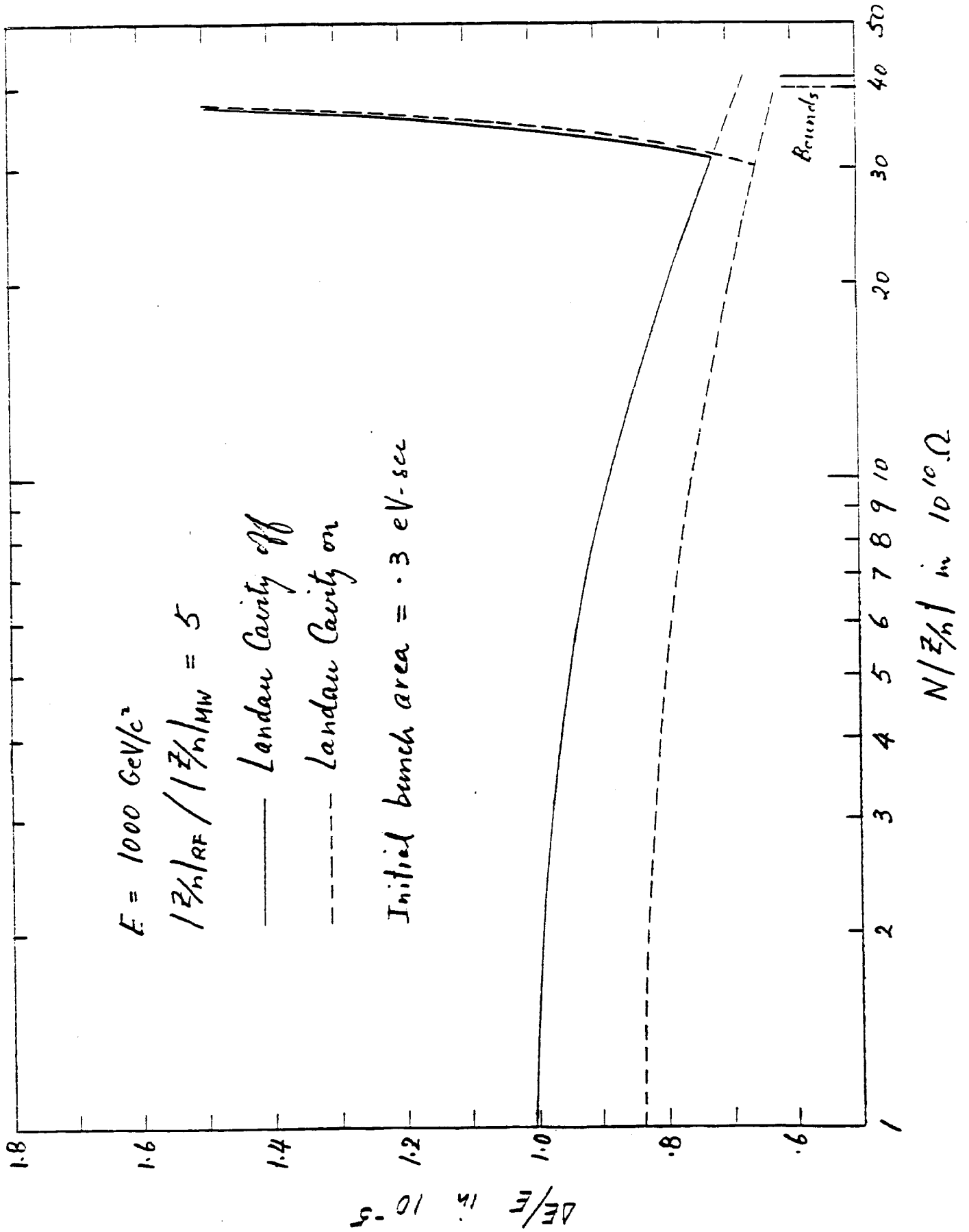


Figure 14

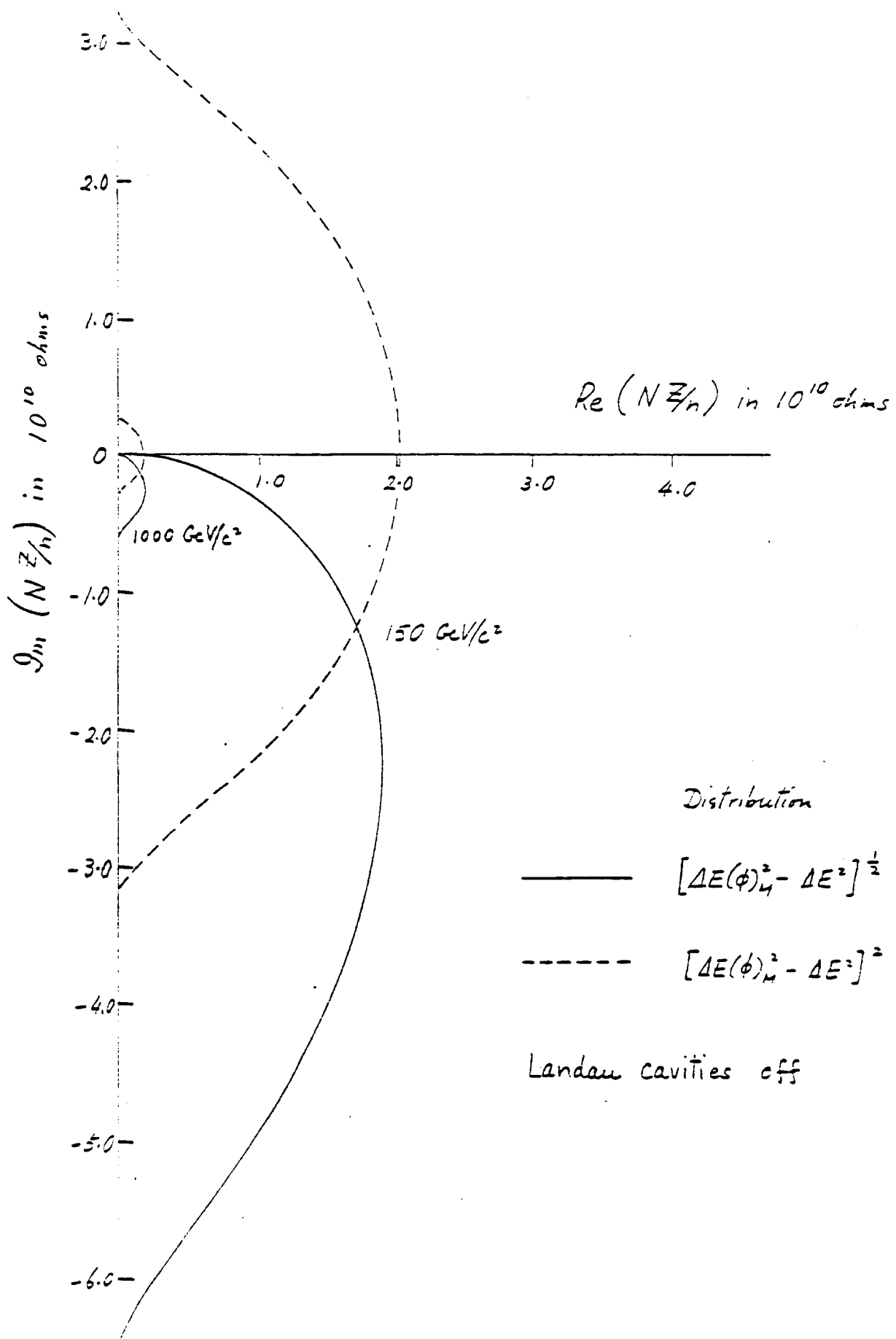
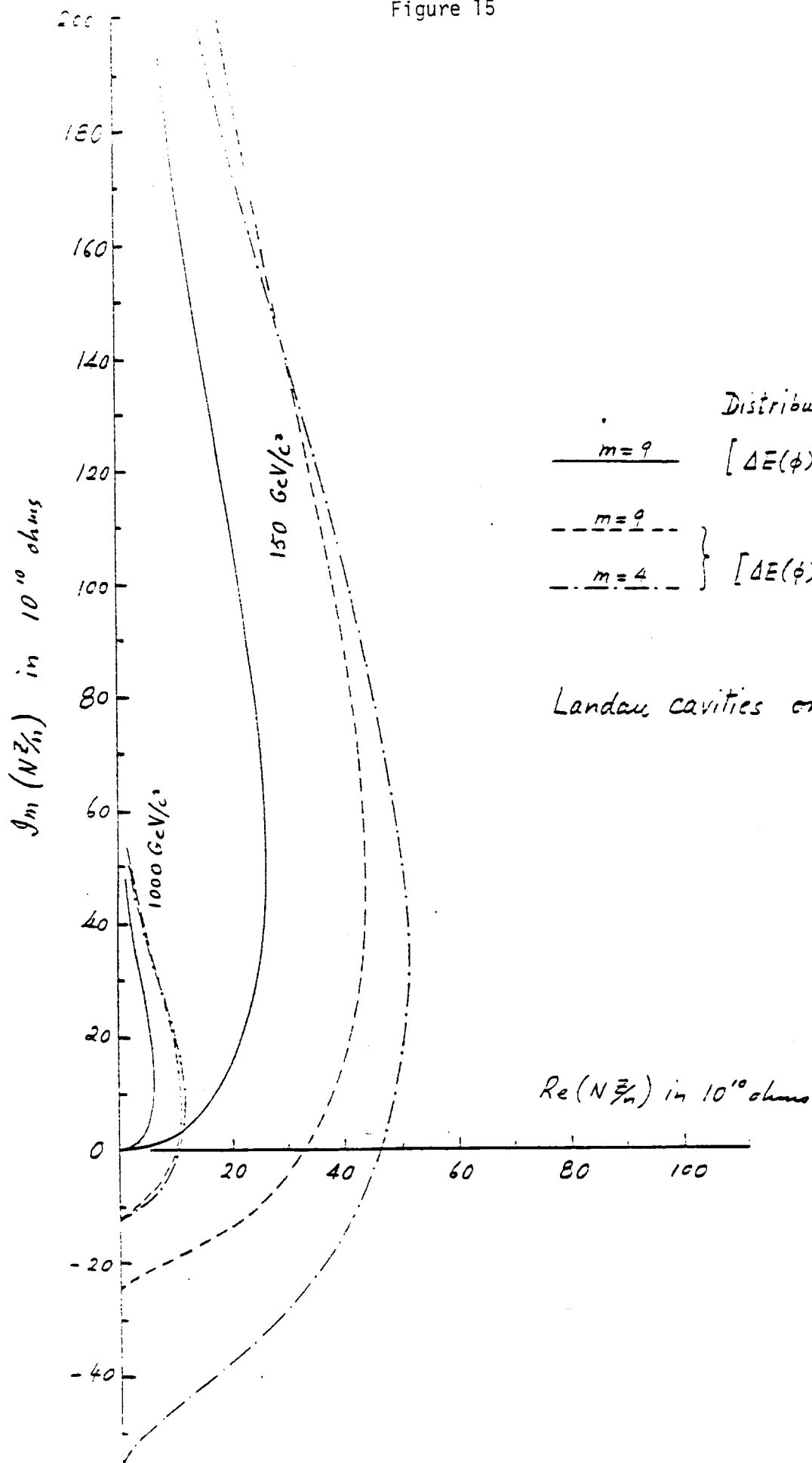


Figure 15



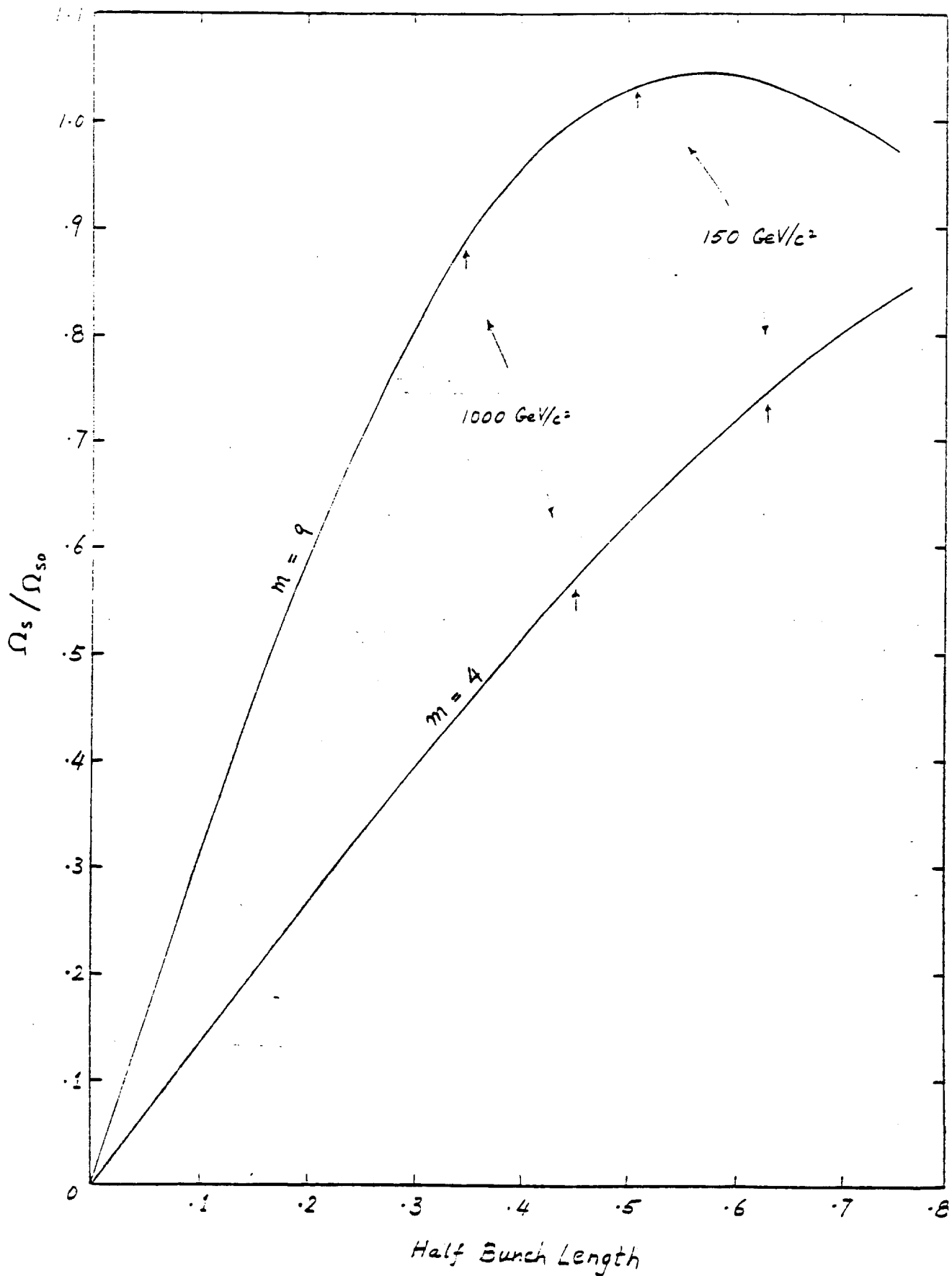
Distribution

$$\frac{m=9}{m=9} \left[\Delta E(\phi)_m^2 - \Delta E^2 \right]^{\frac{1}{2}}$$

$$\left. \begin{array}{l} m=9 \\ m=4 \end{array} \right\} \left[\Delta E(\phi)_m^2 - \Delta E^2 \right]^2$$

Landau cavities on

Figure 16



APPENDIX

In this Appendix, we are going to derive Eq. (5.10).

In the laboratory frame, the perturbing charge density is $e\lambda_1(z-vt)e^{-i\Omega t}$, showing that it travels with velocity $v = \beta c$ around the ring and at the same time oscillates around the bunch with coherent frequency Ω . It can be Fourier analyzed as

$$\begin{aligned} e\lambda_1(z-vt)e^{-i\Omega t} &= e \int d\omega \tilde{\lambda}_1(\omega) e^{-i\omega(t-z/v)-i\Omega t} \\ &= e \int d\omega \tilde{\lambda}_1(\omega-\Omega) e^{-i\omega t+i(\omega-\Omega)z/v}. \end{aligned} \quad (\text{A.1})$$

Due to this perturbing charge density, a particle after passing through a distance dz will have an average increase in potential equal to

$$dV_1 = -eN\beta c dz \int d\omega \frac{Z(\omega)}{2\pi R} \tilde{\lambda}_1(\omega-\Omega) e^{-i\omega t+i(\omega-\Omega)z/v} \quad (\text{A.2})$$

where $Z(\omega)/2\pi R$ is the longitudinal impedance per unit length along the ring. Because the perturbing charge density which causes bunch shape oscillation will be nonvanishing only in the frequency range from the RF to ~ 10 times the RF where $Z(\omega)/\omega$ is almost constant, Eq. (A.2) can be simplified to

$$\begin{aligned} \frac{dV_1}{dz} &\cong -\frac{eN}{2\pi} \frac{Z}{n} \int d\omega \omega \tilde{\lambda}_1(\omega-\Omega) e^{-i\omega t+i(\omega-\Omega)z/v} \\ &= -\frac{ieN}{2\pi} \frac{Z}{n} \frac{\partial}{\partial t} \left[\lambda_1(z-vt) e^{-i\Omega t} \right] \end{aligned} \quad (\text{A.3})$$

with $n = \omega/\omega_0 = \omega R/\beta c$. Since the coherent bunch shape oscillation frequency Ω is very much less than the RF, Eq. (A.3) can be written approximately

$$\frac{dV_1}{dz} \cong \frac{ieN}{2\pi} \frac{Z}{n} \beta c \frac{\partial}{\partial z} \lambda_1(z-vt) e^{-i\omega t}. \quad (\text{A.4})$$

The rate of increase in energy of the particle is

$$\frac{d\Delta E}{dt} = e \frac{dV_1}{dz} \beta c = \frac{ie^2 N v^2}{2\pi} \frac{z}{n} \frac{\partial}{\partial z} \lambda_1(z-vt) e^{-i\Omega t}. \quad (\text{A-5})$$

Going to the frame moving with the synchronous particle, the RF phase is $\phi = -\frac{h}{R}(z-vt)$; the negative sign comes from our convention above transition. Then if we define

$$\frac{d\Delta E}{dt} = -\frac{\omega_0}{2\pi} \frac{\partial \Delta U}{\partial \phi} e^{-i\Omega t}, \quad (\text{A-6})$$

the perturbing Hamiltonian is

$$H_1 = \frac{\omega_0}{2\pi} \Delta U$$

$$= \frac{i\omega_0}{2\pi} e^{2Nh\beta c} \frac{z}{n} \lambda_1(\phi). \quad (\text{A.7})$$